Zeitschrift für Kristallographie 169, 35–49 (1984)

The structure of bytownite (An_{85}). A new refinement

G. Chiari, P. Benna and E. Bruno*

Dipartimento di Scienze della Terra, Università degli Studi di Torino,
Via San Massimo 22, I-10123 Torino

Received: January 18, 1984

Bytownite / Structure refinement

Abstract. Bytownite ($Ca_{0.85}Na_{0.14}Al_{1.83}Si_{2.16}O_8$) ($a$ = 8.188 Å, b = 12.882 Å, c = 14.196 Å, $\alpha = 93.37°$, $\beta = 116.04°$, $\gamma = 90.87°$) from a satellite dyke of the Traversella stock (Italian Western Alps) showing only '*a*' and '*b*' type reflections was refined in space group $I\bar{1}$ using 3756 diffractometer measured intensities. An anisotropic refinement carried out with only Ca/Na split half-atoms gave $R = 0.034$; an alternative model with T and O atoms also treated as isotropic split half-atoms gave $R = 0.038$. Both refinements confirm, in general, the results of the isotropic refinement ($R = 0.118$) by Fleet et al. (1966). The more accurate definition of the atomic coordinates permits discussion of the variations in the Ca/Na cation positions for the average structures of low-temperature calcic plagioclases in the range $An_{50}-An_{100}$. The mean T–O distances in the non-split model ($R = 0.034$) are: $T_1(00) = 1.622$, $T_1(0z) = 1.746$, $T_1(m0) = 1.729$, $T_1(mz) = 1.615$, $T_2(00) = 1.721$, $T_2(0z) = 1.618$, $T_2(m0) = 1.622$, $T_2(mz) = 1.735$ Å. The Al,Si configuration shows a significantly larger degree of order with respect to the An_{85} bytownite thermally treated at 1450 °C (Facchinelli et al., 1979), but if the 7 Å average structure is considered, the degree of order appears identical.

Introduction

The structures of numerous low-temperature calcic plagioclases are known. There are many refinements in the range $An_{90}-An_{100}$ (Kempster et al., 1962; Megaw et al., 1962; Wainwright and Starkey, 1971; Czank, 1973; Berking, 1976) and in the labradorite range ($An_{50}-An_{70}$) (Klein and

---

* To whom correspondence should be sent

Korekawa, 1976; Wenk et al., 1980; Tagai et al., 1980). But in the range $An_{70}-An_{90}$ for bytownite compositions, the only refinement fully published is the one for An_{80} composition by Fleet et al. (1966), who visually estimated the intensities collected using a Weissenberg multiple-film technique. The final *R* value was, for isotropic refinement, 0.118, perhaps not sufficiently accurate by modern standards. To obtain the structural data for a bytownite with the same accuracy as other feldspars we thought it convenient to refine the structure of a plagioclase An_{85}. This refinement should give accurate information in order to allow an interpretation of the structural variations occurring in the range $An_{50}-An_{100}$ in the average structures.

The crystal used in this work has the same composition (An_{85}) and comes from the same satellite dyke of the Traversella stock (Italian Western Alps) as the one thermally treated at 1450 °C, whose structure was refined by Facchinelli et al. (1979). The present refinement permits an accurate comparison of the structures before and after heating.

Hereafter the plagioclase structures to which we more frequently refer will be quoted in the following way: "*low*" plagioclases: AnWS: An_{100} (Wainwright and Starkey, 1971); BytLow: An_{85} (this work); BytL: An_{80} (Fleet et al., 1966); An66: An_{66} (Tagai et al., 1980); "*high*" plagioclases: AnQ: An_{98} (Bruno et al., 1976; Chiari et al., 1978) thermally treated at 1530 °C; BytQ: An_{85} (Facchinelli et al., 1979) thermally treated at 1450 °C.

Experimental details and structure refinement

The chemical composition, determined by microprobe analysis (Facchinelli et al., 1979) is $Ca_{0.85}Na_{0.14}Al_{1.83}Si_{2.16}O_8$. The cell parameters refined from 46 reflections measured on a powder pattern (Guinier camera, CuKα radiation, $\lambda = 1.54178$ Å) are: $a = 8.188(1)$ Å, $b = 12.882(2)$ Å, $c = 14.196(2)$ Å, $\alpha = 93.37(2)°$, $\beta = 116.04(2)°$, $\gamma = 90.87(1)°$. Long-exposure precession and Weissenberg photographs only showed '*a*' ($h + k =$ even, $l =$ even) and '*b*' ($h + k =$ odd, $l =$ odd) reflections. The space group was assumed to be $I\bar{1}$. The crystal dimensions are $0.10 \times 0.20 \times 0.35$ mm.

The intensities were collected using a Nicolet R3 four-circle diffractometer, with graphite-monochromatized MoKα radiation. The ω-scan technique was used with the scanning speed varied from 1.5° min^{-1} for the weakest to 15° min^{-1} for the strongest reflections. The scan range was 1.4° and the background was measured in a stationary mode for half the length of time as the peak was scanned. Two standard reflections were remeasured every 50 observations with no significant variations. An empirical absorption correction based on the ψ-scan method (North et al., 1968) was applied using 4 reflections distributed over the range $12° \leq 2\theta \leq 53°$; the applied absorption coefficients were 1.00–1.26. The reciprocal lattice sphere was explored up to $2\theta = 65°$; 4918 reflections were collected, 3756 of which with $I \geq 3\sigma_I$ were considered as observed and used for the refinement; 2196 of these were '*a*' type, 1564 were '*b*' type reflections; the absence of '*c*' ($h + k =$ even, $l =$ odd) and '*d*' ($h + k =$ odd, $l =$ even) type reflections was confirmed by careful diffractometer measurements. The data were corrected for background and the Lorentz-polarization effect using SHELXTL system (Sheldrick, 1981). Scattering factors were taken from International Tables for X-ray Crystallography (1968). For non-tetrahedral cations, each atom was assumed to be 85% Ca and 15% Na, refining the same positional and thermal parameters by use of the "free variables" provided by the SHELXTL program. In the last cycles of refinement scattering factors for Si and Al were assigned to Si- and Al-rich sites, respectively, obtaining better agreement factors and thermal parameters more similar to one another. For all refinements a weighting scheme was introduced for the final cycles with $w = 1/[\sigma^2(F_o) + G(F_o)^2]$, where σ is the standard deviation of F_o based on counting statistics and G was refined in order to keep $\Sigma w\,(F_o/F_c)^2$ values as constant as possible over ranges of $\sin\theta/\lambda$ and $(F_o/F_{o\,max})^{1/2}$[1].

It is known that in bytownite (Fleet et al., 1966) the presence of $P\bar{1}$ antiphase microdomains, related by the body-centring vector $\frac{1}{2}(a + b + c)$, causes the absence of '*c*' and '*d*' type reflections and simulates the body centred space group.

The average $I\bar{1}$ structure of BytQ was used as starting model. The refinement gave $R = 0.177$ and very pronounced anisotropy of thermal parameters of the two non-tetrahedral cations Ca/Na(0) and Ca/Na(z). The splitting of Ca/Na(0) into two "half-atoms", Ca/Na(000) and Ca/Na(0i0), gave $R = 0.064$. The further splitting of Ca/Na(z) into two "half-atoms", Ca/Na(z00) and Ca/Na(zi0), (with all atoms treated anisotropically), led to $R = 0.034$, $R_w = 0.036$, goodness of fit = 2.04, $G = 0.00015$ for 3756 ('*a*' and '*b*') reflections and 253 least-squares parameters; the maximum residual peak in the difference Fourier map was 0.75 eÅ^{-3}. The R value for the 2192 '*a*' type reflections was 0.027 and for the 1564 '*b*' type reflections was 0.060. Therefore in this model (called the "non-split model" hereafter), the Ca/Na atoms obey $P\bar{1}$ symmetry whereas the framework is body-centred ($I\bar{1}$). Table 1 list the atomic coordinates and the anisotropic thermal parameters obtained for this refinement.

A second model (called the "split model" hereafter) with T and O "half-atoms" was refined using isotropic thermal parameters for these atoms, starting from the coordinates of BytQ split model (see discussion in Facchinelli et al., 1979, for the choice of one of the 2^{25} $P\bar{1}$ 'whole atoms' possible configurations). This model gave: $R = 0.038$, $R_w = 0.042$, goodness of fit = 2.21, $G = 0.00017$. Table 2 lists atomic fractional coordinates, anisotropic thermal parameters for Ca/Na atoms and isotropic thermal parameters for T and O atoms in the $P\bar{1}$ model.

As seen in AnQ (Bruno et al., 1976), the two models are substantially equivalent from the refinement point of view. The split model should be more realistic since to propose a split configuration for the non-tetrahedral cations and a non-split configuration for the T and O atoms would imply that the framework is not at all influenced by the Ca/Na atoms. In Table 3 are listed

---

[1] A list of structure factors can be ordered referring to the no. CSD 51047, names of the authors and citation of the paper at the Fachinformationszentrum Energie-Physik-Mathematik, D-7514 Eggenstein-Leopoldshafen 2, FRG

Table 1. Atomic fractional coordinates (× 10^4), isotropic temperature factors[a] (× 10^3) and anisotropic temperature factors[b] (× 10^3) in the non-split model

	x	y	z	U (Å^2)	U_{11}	U_{22}	U_{33}	U_{23}	U_{13}	U_{12}
Ca/Na(000)	2669(1)	9838(1)	876(1)	20	11(1)	34(1)	15(1)	−9(1)	7(1)	−5(1)
Ca/Na(0i0)	7741(2)	5336(1)	5460(1)	24	14(1)	30(1)	24(1)	−9(1)	4(1)	5(1)
Ca/Na(z00)	2679(4)	310(2)	5435(2)	8	9(1)	9(1)	5(1)	4(1)	3(1)	4(1)
Ca/Na(zi0)	7650(4)	5146(2)	642(2)	42	7(1)	64(2)	41(1)	−38(1)	1(1)	5(1)
T_1(0000)	74(1)	1585(1)	1042(1)	9	9(1)	10(1)	8(1)	1(1)	4(1)	−1(1)
T_1(0z00)	27(1)	1648(1)	6114(1)	8	9(1)	9(1)	8(1)	1(1)	4(1)	−1(1)
T_1(m000)	−4(1)	8154(1)	1189(1)	9	10(1)	9(1)	7(1)	1(1)	4(1)	2(1)
T_1(mz00)	54(1)	8175(1)	6124(1)	9	10(1)	11(1)	7(1)	1(1)	4(1)	3(1)
T_2(0000)	6877(1)	1119(1)	1574(1)	10	8(1)	8(1)	12(1)	1(1)	4(1)	0(1)
T_2(0z00)	6776(1)	1058(1)	6590(1)	11	9(1)	8(1)	14(1)	0(1)	4(1)	0(1)
T_2(m000)	6770(1)	8817(1)	1820(1)	10	9(1)	8(1)	13(1)	3(1)	4(1)	2(1)
T_2(mz00)	6832(1)	8752(1)	6759(1)	9	9(1)	9(1)	11(1)	3(1)	5(1)	1(1)
O_A(1000)	98(2)	1259(1)	9916(1)	18	28(1)	18(1)	10(1)	2(1)	11(1)	0(1)
O_A(1z00)	−78(2)	1259(1)	4876(1)	18	30(1)	17(1)	13(1)	3(1)	14(1)	4(1)
O_A(2000)	5771(2)	9904(1)	1401(1)	13	11(1)	11(1)	15(1)	4(1)	5(1)	3(1)
O_A(2z00)	5730(2)	9915(1)	6373(1)	12	10(1)	10(1)	16(1)	2(1)	4(1)	0(1)
O_B(0000)	8191(2)	1010(1)	897(1)	19	15(1)	15(1)	29(1)	−4(1)	14(1)	−5(1)
O_B(0z00)	8019(2)	1015(1)	5960(1)	19	17(1)	15(1)	32(1)	−2(1)	16(1)	−3(1)
O_B(m000)	8107(3)	8550(1)	1294(2)	29	20(1)	21(1)	54(1)	−5(1)	24(1)	2(1)
O_B(mz00)	8193(2)	8554(1)	6122(2)	24	19(1)	22(1)	38(1)	2(1)	20(1)	5(1)
O_C(0000)	126(2)	2800(1)	1357(1)	16	16(1)	12(1)	20(1)	−1(1)	9(1)	−2(1)
O_C(0z00)	142(2)	2948(1)	6479(1)	16	16(1)	13(1)	18(1)	−0(1)	7(1)	−3(1)
O_C(m000)	87(2)	6807(1)	1083(1)	15	13(1)	13(1)	15(1)	1(1)	4(1)	4(1)
O_C(mz00)	84(2)	6919(1)	6001(1)	16	18(1)	13(1)	15(1)	−0(1)	4(1)	4(1)
O_D(0000)	1894(2)	1063(1)	1881(1)	18	15(1)	17(1)	14(1)	2(1)	−0(1)	3(1)
O_D(0z00)	2041(2)	1040(1)	6903(1)	20	18(1)	14(1)	16(1)	2(1)	−2(1)	2(1)
O_D(m000)	2000(2)	8690(1)	2177(1)	24	16(1)	20(1)	21(1)	−6(1)	−5(1)	2(1)
O_D(mz00)	1833(3)	8620(1)	7128(1)	29	23(1)	23(1)	22(1)	−7(1)	−8(1)	4(1)

[a] Equivalent isotropic U defined as one third of the trace of the orthogonalised U_{ij} tensor

[b] The anisotropic temperature factor exponent takes the form: $-2\pi^2(h^2a^{*2}U_{11}+k^2b^{*2}U_{22}+l^2c^{*2}U_{33}+2klb^*c^*U_{23}+2hla^*c^*U_{13}+2hka^*b^*U_{12})$

Table 2. Atomic fractional coordinates ($\times 10^4$), anisotropic temperature factors ($\times 10^3$) of Ca/Na atoms and isotropic temperature factors ($\times 10^3$) of T and O atoms in the $P\bar{1}$ model

	x	y	z	U(Å^2)	U_{11}	U_{22}	U_{33}	U_{23}	U_{13}	U_{12}
Ca/Na(000)	2669(2)	9838(2)	876(1)	20(1)	10(1)	34(1)	15(1)	−10(1)	7(1)	−5(1)
Ca/Na(0i0)	7742(2)	5336(1)	5460(1)	24(1)	13(1)	29(1)	24(1)	−9(1)	4(1)	5(1)
Ca/Na(z00)	2680(4)	310(2)	5436(2)	8(1)	9(1)	9(1)	5(1)	4(1)	3(1)	4(1)
Ca/Na(zi0)	7648(4)	5146(3)	641(2)	42(1)	6(1)	62(2)	41(2)	−38(1)	1(1)	5(1)

	x	y	z	U(Å^2)		x	y	z	U(Å^2)
T$_1$(0000)	30(5)	1624(3)	1035(3)	14(1)	O$_B$(0000)	8103(4)	1041(3)	804(3)	13(1)
T$_1$(00i0)	5107(1)	6555(1)	6046(1)	3(1)	O$_B$(00i0)	3279(4)	5980(3)	5988(3)	12(1)
T$_1$(0z00)	63(5)	1614(3)	6110(3)	8(1)	O$_B$(0z00)	8110(6)	995(4)	6057(4)	10(1)
T$_1$(0zi0)	4992(5)	6681(3)	1118(3)	6(1)	O$_B$(0zi0)	2918(7)	6039(4)	852(4)	15(1)
T$_1$(m000)	9929(5)	8119(3)	1178(3)	9(1)	O$_B$(m000)	8206(5)	8522(3)	1426(3)	14(1)
T$_1$(m0i0)	5057(4)	3187(3)	6199(3)	5(1)	O$_B$(m0i0)	3003(5)	3579(3)	6156(3)	18(1)
T$_1$(mz00)	114(2)	8217(1)	6133(1)	7(1)	O$_B$(mz00)	8095(4)	8545(3)	6023(3)	12(1)
T$_1$(mzi0)	4992(2)	3132(1)	1114(1)	8(1)	O$_B$(mzi0)	3309(5)	3566(3)	1239(3)	20(1)
T$_2$(0000)	6876(4)	1109(2)	1524(2)	7(1)	O$_C$(0000)	57(4)	2819(2)	1298(2)	10(1)
T$_2$(00i0)	1877(4)	6128(2)	6625(2)	8(1)	O$_C$(00i0)	5204(5)	7781(3)	6423(3)	17(1)
T$_2$(0z00)	6790(4)	1053(2)	6645(2)	8(1)	O$_C$(0z00)	189(5)	2927(3)	6455(3)	16(1)
T$_2$(0zi0)	1762(4)	6064(2)	1532(2)	9(1)	O$_C$(0zi0)	5098(11)	7969(7)	1503(7)	13(2)
T$_2$(m000)	6769(2)	8831(1)	1875(1)	9(1)	O$_C$(m000)	24(4)	6773(3)	1110(3)	13(1)
T$_2$(m0i0)	1771(2)	3803(1)	6767(1)	7(1)	O$_C$(m0i0)	5148(4)	1841(2)	6054(2)	11(1)
T$_2$(mz00)	6801(5)	8727(3)	6714(3)	8(1)	O$_C$(mz00)	183(5)	6955(3)	5976(3)	14(1)
T$_2$(mzi0)	1862(5)	3777(3)	1804(3)	7(1)	O$_C$(mzi0)	4992(4)	1886(2)	1023(2)	10(1)
O$_A$(1000)	250(4)	1250(2)	9950(2)	11(1)	O$_D$(0000)	1811(4)	1053(3)	1922(3)	13(1)
O$_A$(10i0)	4935(5)	6270(3)	4881(3)	14(1)	O$_D$(00i0)	6979(5)	6075(3)	6839(3)	14(1)
O$_A$(1z00)	9756(4)	1237(3)	4830(3)	12(1)	O$_D$(0z00)	2142(4)	1044(2)	6852(2)	10(1)
O$_A$(1zi0)	5086(4)	6281(3)	9922(3)	13(1)	O$_D$(0zi0)	6930(5)	6035(3)	1959(3)	15(1)
O$_A$(2000)	5774(4)	9924(2)	1455(2)	8(1)	O$_D$(m000)	2079(4)	8722(2)	2108(2)	11(1)
O$_A$(20i0)	768(4)	4883(3)	6341(3)	13(1)	O$_D$(m0i0)	6908(5)	3653(3)	7254(3)	18(1)
O$_A$(2z00)	5736(4)	9901(3)	6311(3)	13(1)	O$_D$(mz00)	1721(4)	8581(3)	7197(3)	12(1)
O$_A$(2zi0)	727(4)	4928(2)	1425(2)	7(1)	O$_D$(mzi0)	6966(5)	3662(3)	2051(3)	19(1)

Table 3. Split lengths between the two half-atoms obtained applying the body-centring vector to one atom of the pair in BytLow (split model) and in AnWS. For T and O atoms the mean values are reported

	Ca/Na(000)	Ca/Na(z00)	T_1	T_2	$O_A(1)$	$O_A(2)$	O_B	O_C	O_D
BytLow	0.915	0.379	0.121	0.145	0.241	0.167	0.291	0.175	0.294
AnWS	0.953	0.586	0.087	0.188	0.280	0.082	0.371	0.103	0.395

the values of the split between atoms related by the pseudo-symmetry vector $\frac{1}{2}(a + b + c)$ for BytLow, together with the corresponding values for AnWS for comparison. From Table 3 the following variations of the splits of BytLow with respect to AnWS can be evinced:

a) a drastic decrease in the Ca/Na(z00) − Ca/Na(zi0) split;

b) an increase of the split for the T_1 sites and decrease for the T_2 sites;

c) a decrease of the split values for $O_A(1)$, O_B and O_D and a significant increase for $O_A(2)$ and O_C atoms.

The split for T and O atoms are, in general, of the same order of magnitude for the two structures. This should favour the choice of a split model for BytLow. However, the choice of a $P\bar{1}$ configuration, done on the basis of the analogy with AnWS, leads to tetrahedra showing a very pronounced degree of distortion. Furthermore, the sum of Al-occupancies of the T sites obtained for the non-split model is closer to the results of the microprobe analysis. This is probably related to the ambiguity of the choice for those atoms for which either the split is small or is oriented in a different way with respect to AnWS. Not being positive about the choice of a unique $P\bar{1}$ configuration, we adopted the model with T and O atoms in the non-split configuration. On the basis of these observations the choice of the split model made by Facchinelli et al. (1979) for BytQ can be challenged as well. The model used in the next paragraphs is therefore represented by an $I\bar{1}$ average framework configuration and by a $P\bar{1}$ configuration for the non-tetrahedral cations. The thermal ellipsoids for the T and O atoms of this model are, at least in part, average in space of the two close half-atoms related by the pseudo-symmetry vector. Table 4 shows the root-mean-square displacements. Table 5 − 8 show the relevant distances and angles. E.s.d.'s are 0.001 and 0.002 Å for Ca/Na − O and T − O lengths, respectively and 0.1° for O − T − O and T − O − T angles.

Discussion

Ca/Na environment

In order to compare the Ca/Na positions determined in the four sub-cells of BytLow with the corresponding ones in the structures of the low calcic

Table 4. Root-mean-square displacements (× 10^3 Å)

	1	2	3		1	2	3
Ca/Na(000)	101	199	93	O_A(2000)	111	129	89
Ca/Na(0i0)	127	207	105	O_A(2z00)	99	129	96
Ca/Na(z00)	85	110	54	O_B(0000)	124	176	88
Ca/Na(zi0)	105	329	76	O_B(0z00)	121	182	97
T_1(0000)	91	104	82	O_B(m000)	143	235	92
T_1(0z00)	111	120	100	O_B(mz00)	150	194	92
T_1(m000)	108	125	102	O_C(0000)	123	144	101
T_1(mz00)	86	110	82	O_C(0z00)	132	133	101
T_2(0000)	110	130	106	O_C(m000)	118	139	95
T_2(0z00)	91	119	87	O_C(mz00)	114	156	103
T_2(m000)	95	119	80	O_D(0000)	129	161	96
T_2(mz00)	110	126	106	O_D(0z00)	116	187	94
O_A(1000)	131	165	81	O_D(m000)	133	211	89
O_A(1z00)	129	173	85	O_D(mz00)	141	238	95

Table 5. Ca/Na – O interatomic distances (Å)

	Ca/Na(000)	Ca/Na(0i0)		Ca/Na(z00)	Ca/Na(zi0)
O_A(1000)	2.745	2.327	O_A(1z00)	2.418	2.525
O_A(100c)	2.424	2.924	O_A(1z0c)	2.785	2.573
O_A(2000)	2.310	2.338	O_A(2z00)	2.339	2.299
O_A(2z0c)	3.525*	>4*	O_A(2z0c)	3.351*	3.641*
O_A(200c)	3.991*	3.362*	O_A(200c)	>4*	>4*
O_B(000c)	2.474	2.362	O_B(0z0c)	2.397	2.489
O_B(m00c)	3.644*	2.771	O_B(mz0c)	2.562	2.926
O_C(0z00)	3.103	3.691*	O_C(0000)	3.817*	3.607*
O_C(mz00)	3.256*	2.614	O_C(m000)	2.557	2.751
O_D(0000)	2.344	2.541	O_D(0z00)	2.499	2.311
O_D(m000)	2.661	3.559	O_D(mz00)	3.609*	3.232*

* Assumed to be non bonded

plagioclases available today the *y* and *z* coordinates of the non-tetrahedral cations are plotted in Figure 1 in the range $An_{50}-An_{100}$. The shift of Ca/Na(zi0) is the most meaningful; this site progressively moves from An_{100} to An_{66}, to join the location of the (z00) site for this last composition. The joint position for (z00) and (zi0) further merges with the (0i0) site for An_{52}. The decrease in the Ca/Na(z00) – Ca/Na(zi0) split from 0.586 Å in AnWS to 0.379 Å in BytLow (see Table 3) is therefore ascribable to the shift of the (zi0) site. The open symbols in Figure 1, referring to BytL, were not considered in the drawing of the lines joining the points, since the *y* coordinate of the (0i0) and (z00) sites results inverted with respect to the general trend of the other plagioclases. This disagreement may be due to the high *R* value of the

Table 6. T – O bond length (Å) and Δ_{tet}[a] ($\times 10^2$)

T_1(0000)	– O_A(1000)	1.637	T_1(0z00)	– O_A(1z00)	1.763
	O_B(0000)	1.624		O_B(0z00)	1.743
	O_C(0000)	1.597		O_C(0z00)	1.713
	O_D(0000)	1.631		O_D(0z00)	1.763
	Mean	1.622		Mean	1.746
	Δ_{tet}	0.009		Δ_{tet}	0.014
T_1(m000)	– O_A(1000)	1.753	T_1(mz00)	– O_A(1z00)	1.641
	O_B(m000)	1.701		O_B(mz00)	1.607
	O_C(m000)	1.738		O_C(mz00)	1.619
	O_D(m000)	1.723		O_D(mz00)	1.593
	Mean	1.729		Mean	1.615
	Δ_{tet}	0.012		Δ_{tet}	0.012
T_2(0000)	– O_A(2000)	1.745	T_2(0z00)	– O_A(2z00)	1.636
	O_B(0000)	1.732		O_B(0z00)	1.622
	O_C(mz00)	1.725		O_C(m000)	1.616
	O_D(mz00)	1.683		O_D(m000)	1.599
	Mean	1.721		Mean	1.618
	Δ_{tet}	0.018		Δ_{tet}	0.007
T_2(m000)	– O_A(2000)	1.640	T_2(mz00)	– O_A(2z00)	1.750
	O_B(m000)	1.604		O_B(mz00)	1.729
	O_C(0z00)	1.609		O_C(0000)	1.716
	O_D(0z00)	1.634		O_D(0000)	1.744
	Mean	1.622		Mean	1.735
	Δ_{tet}	0.009		Δ_{tet}	0.006

[a] $\Delta_{tet} = \frac{1}{4}\Sigma_{i=1}^{4}[(l_i - \bar{l})/\bar{l}]^2$ (Brown and Shannon, 1973)

Table 7. Bond angles at tetrahedral T atoms (°)

	$O_A - O_B$	$O_A - O_C$	$O_A - O_D$	$O_B - O_C$	$O_B - O_D$	$O_C - O_D$
T_1(0000)	102.1	117.0	102.6	111.1	113.5	110.2
T_1(0z00)	98.4	119.2	98.2	112.9	115.1	111.9
T_1(m000)	104.2	113.0	102.3	112.9	113.7	110.2
T_1(mz00)	102.3	113.1	105.8	112.1	113.6	109.7
T_2(0000)	106.4	102.4	107.5	112.5	111.7	115.4
T_2(0z00)	106.9	101.7	110.0	112.6	111.1	113.9
T_2(m000)	109.9	105.3	109.0	111.9	109.0	111.7
T_2(mz00)	108.1	105.5	105.4	111.0	112.0	114.4

Table 8. Bond angles at oxygen atoms (°)

	O_A		O_B	O_C	O_D
1000	139.4	0000	133.8	131.9	133.3
1z00	137.2	0z00	135.4	131.1	128.1
2000	125.5	m000	159.2	130.9	147.7
2z00	124.3	mz00	150.3	129.3	154.1

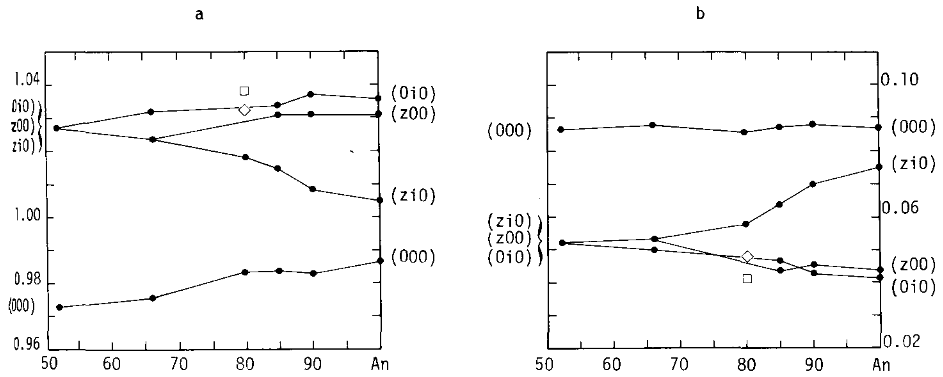

Fig. 1. (a) *y* and (b) *z* coordinates of the Ca/Na atoms in the range $An_{50}-An_{100}$. An_{52}: Klein and Korekawa (1976); An_{66}: An66; An_{80}: BytL [*square*: Ca/Na(z00), *rhomb*: Ca/Na(0i0)]; An_{85}: BytLow; An_{90}: Berking (1976); An_{100}: AnWS

refinement of BytL. The coordinates of the other sites agree with the general trend displayed in Figure 1.

The most significant difference between BytLow and BytQ introduced by the thermal treatment is the non-convergence of the (zi0) site for BytQ toward the single average position observed in Figure 1 for the low-temperature plagioclases. New data on the positions of the non-tetrahedral sites in the more Na-rich plagioclases are necessary to define the trend for the high-temperature series.

In Figure 2 the non-tetrahedral cations and the O_B and O_D atoms are projected onto the plane (100) along a^*. Data for An66, for BytLow and for AnWS are shown. The body-centering vector was applied to the Ca/Na atoms in Figure 2b and also to the oxygen atoms in Figure 2c. The displacement of the (zi0) site in the $An_{66}-An_{100}$ range also explains the electron density distribution around the non-tetrahedral cations found in An66 by Wenk et al. (1980). The position of the (zi0) site close to the (z00) and (0i0) sites may explain, in a 7 Å average structure, the existence in the Fourier map of a larger peak with coordinates $y \sim 0.03$, $z \sim 0.10$ and a smaller peak with coordinates $y \sim 0.98$, $z \sim 0.16$. Therefore the first of the two split positions refined by Wenk et al. (1980) corresponds to the average position of the (z00), (zi0) and (0i0) sites; the second one to the (000) site alone.

Since the configuration of the oxygen atoms around the (000) site in calcic plagioclases is very similar to the one around the Na atom in low albite, one may suspect that there is a tendency for the Na atom to preferencially concentrate in this site, even though no clear suggestions in this sense can be inferred from the refinements. Although unproven, this hypothesis is attractive since it may explain the fact that the (000) site does not merge with the other non-tetrahedral sites for the composition An_{52}.

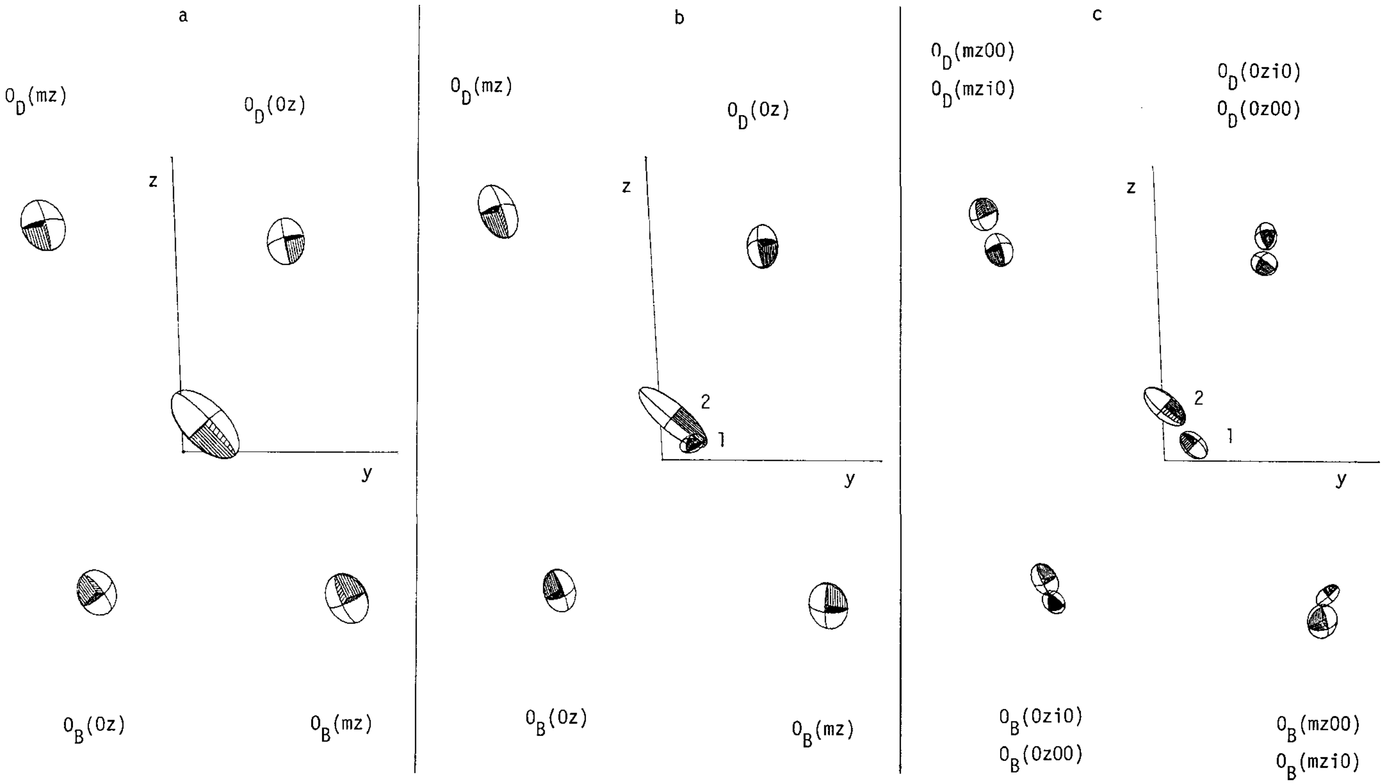

Fig. 2. Projection down a^* in the yz plane of Ca/Na, O_D and O_B atoms. The origin of the drawing is: $x=0.65$, $y=0.50$, $z=0$. (a) An66: Ca/Na(z); (b) BytLow: 1 = Ca/Na(z00), 2 = Ca/Na(zi0); (c) AnWs: 1 = Ca(z00), 2 = Ca(zi0). The body-centering vector was applied when necessary to one sub-cell to compare the three structures

Table 9. Al-occupancies (t)[a] in the tetrahedral sites in BytQ and BytLow

	BytQ	BytLow
$t_1(0000)$	0.19	0.05
$t_1(0z00)$	0.89	1.00
$\langle t_1(0)\rangle$	0.54	0.52
$t_1(m000)$	0.74	0.87
$t_1(mz00)$	0.14	0.00
$\langle t_1(m)\rangle$	0.44	0.43
$t_2(0000)$	0.74	0.81
$t_2(0z00)$	0.12	0.02
$\langle t_2(0)\rangle$	0.43	0.41
$t_2(m000)$	0.13	0.05
$t_2(mz00)$	0.76	0.91
$\langle t_2(m)\rangle$	0.45	0.48
ΔAl[b]	0.10	0.08

[a] $t_i = 0.25\,(1 + n_{An}) + (\langle T_i-O\rangle - \langle\!\langle T-O\rangle\!\rangle)/0.13$ (Kroll and Ribbe, 1983)

[b] $\Delta Al = t_1(0) - 1/3\,[t_1(m) + t_2(0) + t_2(m)]$ (Ribbe, 1975b)

Al,Si configurations

The Al-occupancies of the T sites, calculated according to Kroll and Ribbe (1983) and reported in Table 9, are not significantly different from those obtained from the dimensions of the tetrahedra of BytL. It is interesting to speculate whether or not the degree of order observed in BytLow is the maximum observable in a low temperature plagioclase of composition An_{85}. If the plagioclases are considered as a "mechanical mixture" of low albite- and anorthite-like domains (Smith and Ribbe, 1969), the Al,Si distribution expected for the An_{85} composition in the 7 Å average structure (Ribbe, 1975a) is $t_1(0) = 0.575$, $t_1(m) = t_2(0) = t_2(m) = 0.425$ and ΔAl (Ribbe, 1975b) $= t_1(0) - 1/3\,[t_1(m) + t_2(0) + t_2(m)] = 0.15$, while in BytLow $\Delta Al = 0.08$.

It is well known that the ordering schemes of albite and anorthite are topochemically incompatible in a single continuous framework without interposing disordered boundaries between An and Ab domains (Ribbe, 1975a). These disordered boundaries explain the lower degree of order found in BytLow and in all structures of low plagioclases in the whole range Ab–An with respect to that expected from the mechanical mixture model. Moreover the good agreement of the Al-occupancies observed in BytLow with those obtained for BytL, may suggest that in these two plagioclases the observed distributions correspond to the maximum possible order for these compositions. If not, the two plagioclases under examination, coming from different geological environments would show, by chance, the same degree of

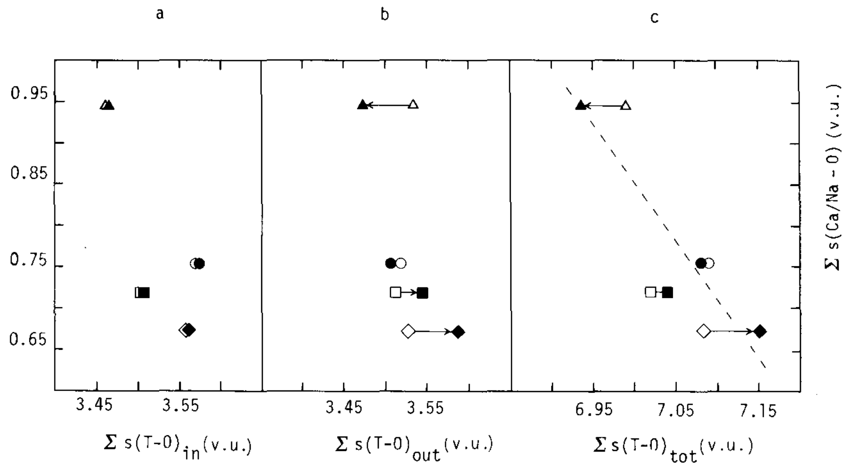

Fig. 3. Ca/Na—O bond-strength sums to the four O atoms of each tetrahedron plotted *versus* T—O bond strength sums for BytLow. The T atoms internal to the tetrahedron are considered in (a), the T atoms of neighbouring tetrahedra in (b) and all T atoms in (c). Each point represents the average of the four tetrahedra of the average site: $T_1(0)$ *triangles*, $T_2(0)$ *circles*, $T_2(m)$ *squares*, $T_1(m)$ *rhombs*. Open symbols: undistorted tetrahedra; filled symbols: actual tetrahedra

order, and therefore, an identical thermal history. This cannot, of course, be excluded in principle, but seems unlikely.

Table 9 allows a comparison among the different Al,Si configurations in BytLow and in BytQ. If the individual tetrahedra of the 14 Å structures are considered, a larger degree of order in BytLow appears. On the contrary, if the 7 Å average structures are considered, the Al-occupancies in the four T sites and the ΔAl value are almost identical for BytLow and BytQ. This identity is a consequence of the averaging. On the other hand, it is known that the variation of the cell angle γ (and γ-related parameters) in a low and high plagioclases is related to the degree of order in the 7 Å average structure (i.e. ΔAl) (Kroll, 1978; Bruno and Facchinelli, 1979; Kroll and Ribbe, 1980). The similar ΔAl values in BytLow and BytQ confirm the interpretation given by Bruno and Facchinelli (1979) to the variations of the cell parameters in low- and high-temperature plagioclases in the $An_{70}-An_{100}$ range.

Facchinelli et al. (1979) emphasize the correlation between the Al-occupancies and the Ca/Na—O bond strengths in BytQ. It could be interesting to compare the role played by Al-occupancies in BytLow and BytQ for the achievement of the charge balance. The Ca/Na—O bond strengths *versus* T—O bond strengths for BytLow and BytQ (non-split model) are plotted in Figure 3 and Figure 4 respectively.

The parameters are the same already used in previous papers (Chiari et al., 1978; Facchinelli et al., 1979) and are only summarized here, since a more detailed explanation is given in the

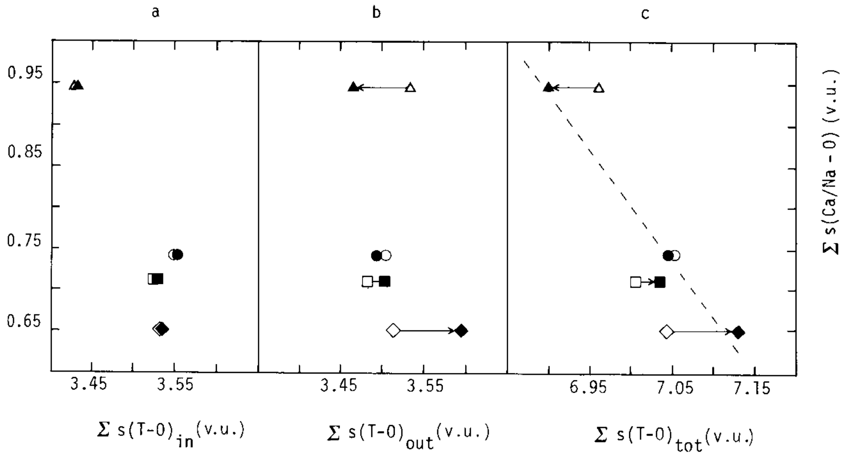

Fig. 4. Ca/Na – O bond-strength sums to the four O atoms of each tetrahedron plotted *versus* T – O bond-strength sums for BytQ (non-split model). (See Fig. 3 caption)

quoted papers: $\Sigma s(\mathrm{Ca/Na-O})$ = bond strengths sums from Ca/Na atoms; $\Sigma s(\mathrm{T-O})_{\mathrm{in}}$ = bond strength sums from T atoms inside the tetrahedron; $\Sigma s(\mathrm{T-O})_{\mathrm{out}}$ = bond strength sums from T atoms outside the tetrahedron; $\Sigma s(\mathrm{T-O})_{\mathrm{tot}} = \Sigma s(\mathrm{T-O})_{\mathrm{in}} + \Sigma s(\mathrm{T-O})_{\mathrm{out}}$. The bond strengths were calculated following Brown and Wu (1976), using the actual T – O distances (distorted) and the average T – O for a given tetrahedron (undistorted).

Figure 3 shows that:

3c: the global contribution to the bond strengths from the T cations [$\Sigma s(\mathrm{T-O})_{\mathrm{tot}}$] is strongly correlated ($r^2_{\mathrm{distorted}} = 0.94$) with the $\Sigma s(\mathrm{Ca/Na-O})$ and therefore the charge balance can be considered satisfactory;

3b: the good correlation ($r^2_{\mathrm{distorted}} = 0.89$) of $\Sigma s(\mathrm{T-O})_{\mathrm{out}}$ with $\Sigma s(\mathrm{Ca/Na-O})$ can be explained on the basis of the distortion of the tetrahedra;

3a: the correlation of the $\Sigma s(\mathrm{T-O})_{\mathrm{in}}$ (i.e. Al-occupancy) with the $\Sigma s(\mathrm{Ca/Na-O})$ is moderate ($r^2_{\mathrm{undistorted}} = 0.78$), but significant.

In BytQ (Fig. 4) the trend is almost the same and the correlation coefficients are: 4c) $r^2_{\mathrm{distorted}} = 0.97$; 4b) $r^2_{\mathrm{distorted}} = 0.78$; 4a) $r^2_{\mathrm{undistorted}} = 0.92$. Therefore the Al-occupancy and the distortion of the tetrahedra contribute together to the achievement of the charge balance.

The correlations reported in Figure 3 and 4 can lead to conclude that the different Ca/Na – O bond strengths on the oxygen atoms of the different tetrahedra control the average Al,Si configuration in the 7 Å average structures. The identity of ΔAl values could appear, in this way, justified and one could therefore conclude that the thermal treatment does not modify the Al,Si distribution. As already pointed out, this identity is due to the averaging. Actually the thermal treatment induces a considerable degree of disorder, if the 14 Å structure is considered. As mentioned above, in the low-temperature structure the Al-occupancies in the T sites represent the average of the Al,Si configurations in the low albite-like domains, in the anorthite-like domains as well as in the disordered boundaries. The modification induced by the thermal treatment on this configuration is significant and the high-temperature structure can be considered as a compromise between the Al,Si disorder required at high temperature [with the limit imposed by the Loewenstein's (1954) Al-avoidance rule] and the Al,Si configuration required to balance the different Ca/Na – O bond strength contributions to the tetrahedra.

Acknowledgement. This work was supported by Ministero della Pubblica Istruzione and C.N.R. – Roma.

References

Berking, B.: Die Verfeinerung der Kristallstruktur eines lunaren Plagioklases An_{90}. Z. Kristallogr. **144**, 189 – 197 (1976)

Brown, I. D., Shanno R. D.: Empirical bond-strength bond-length curves for oxides. Acta Crystallogr. **A29**, 266 – 282 (1973)

Brown, I. D., Wu, K. K.: Empirical parameters for calculating cation-oxygen bond valences. Acta Crystallogr. **B32**, 1957 – 1959 (1976)

Bruno, E., Facchinelli, A.: Al – Si order-disorder and cell parameters in calcic plagioclases. Rendiconti Soc. Ital. Min. Petrol. **35**, 59 – 70 (1979)

Bruno, E., Chiari, G., Facchinelli, A.: Anorthite quenched from 1530 °C. I. Structure refinement. Acta Crystallogr. **B32**, 3270 – 3280 (1976)

Chiari, G., Facchinelli, A., Bruno, E.: Anorthite quenched from 1530 °C. II. Discussion. Acta Crystallogr. **B34**, 1757 – 1764 (1978)

Czank, M.: Strukturen des Anorthits bei höheren Temperaturen. Thesis, E.T.H., Zürich (1973)

Facchinelli, A., Bruno, E., Chiari, G.: The structure of bytownite quenched from 1723 K. Acta Crystallogr. **B35**, 34 – 42 (1979)

Fleet, S. G., Chandrasekhar, S., Megaw, H. D.: The structure of bytownite ('body-centred anorthite'). Acta Crystallogr. **21**, 782 – 801 (1966)

International Tables for X-ray Crystallography. Vol. III (1968)

Kempster, C. J. E., Megaw, H. D., Radoslovich, E. W.: The structure of anorthite $CaAl_2Si_2O_8$. I. Structure analysis. Acta Crystallogr. **15**, 1005 – 1017 (1962)

Klein, S., Korekawa, M.: Die gemittelte Struktur des Labradorits. N. Jahrb. Miner. Mh. **H2**, 66 – 69 (1976)

Kroll, H.: The structures of heat-treated plagioclases An_{28}, An_{52}, An_{69} and the estimation of Al,Si order from lattice parameters. Phys. Chem. Minerals **3**, 76 – 77 (1978)

Kroll, H., Ribbe, P.H.: Determinative diagrams for Al,Si order in plagioclases. Am. Mineral. **65**, 449 – 457 (1980)

Kroll, H., Ribbe, P. H.: Lattice parameters, composition and Al,Si order in alkali feldspars. In: *Feldspar Mineralogy* (Ed. P. H. Ribbe), Reviews in Mineralogy, vol. 2, second edition, p. 57 – 99. Blacksburg: Southern Printing Co. (1983)

Loewenstein, W.: The distribution of aluminum in the tetrahedral of silicates and aluminates. Am. Mineral. **39**, 92 – 96 (1954)

Megaw, H. D., Kempster, C. J. E., Radoslovich, E. W.: The structure of anorthite, $CaAl_2Si_2O_8$. II. Description and discussion. Acta Crystallogr. **15**, 1017 – 1035 (1962)

North, A. C. T., Phillips, D. C., Mathews, F. S.: A semi-empirical method of absorption correction. Acta Crystallogr. **A24**, 351–359 (1968)

Ribbe, P. H.: The chemistry, structure and nomenclature of feldspars. In: *Feldspar Mineralogy*, M. S. A. Shourt Course Notes (Ed. P. H. Ribbe), p. R1–R51. Blacksburg: Southern Printing Co. (1975a)

Ribbe, P. H.: Optical properties and lattice parameters of plagioclase feldspars. In: *Feldspar Mineralogy*, M. S. A. Short Course Notes (Ed. P. H. Ribbe), p. R53–R72. Blacksburg: Southern Printing Co. (1975b)

Sheldrick, G. M.: SHELXTL, revision 3. An integrated system for solving, refining and displaying crystal structures from diffraction data. Univ. of Göttingen (1981)

Smith, J. V., Ribbe, P. H.: Atomic movements in plagioclase feldspars: kinetic interpretation. Contrib. Mineral. Petrol. **21**, 157–202 (1969)

Tagai, T., Joswig, W., Korekawa, M., Wenk, H. R.: Die Bestimmung der Al/Si-Verteilung mittels Neutronenbeugung in einen Plagioklas An_{66}. Z. Kristallogr. **151**, 77–89 (1980)

Wainwright, J. E., Starkey, J.: A refinement of the structure of anorthite. Z. Kristallogr. **133**, 75–84 (1971)

Wenk, H. R., Joswig, W., Tagai, T., Korekawa, M., Smith, B. K.: The average structure of An_{62-66} labradorite. Am. Mineral. **65**, 81–95 (1980)